

Electron Captures and Stability of White Dwarfs

N. Chamel*, L. Perot

*Institut d'Astronomie et d'Astrophysique, Université Libre de Bruxelles,
CP-226, 1050 Brussels, Belgium
E-mail: nicolas.chamel@ulb.be

A. F. Fantina

*Grand Accélérateur National d'Ions Lourds (GANIL), CEA/DRF - CNRS/IN2P3, Boulevard
Henri Becquerel, 14076 Caen, France*

*Institut d'Astronomie et d'Astrophysique, CP-226, Boulevard du Triomphe, Université Libre de
Bruxelles, 1050 Brussels, Belgium*

D. Chatterjee, S. Ghosh

*Inter-University Centre for Astronomy and Astrophysics, Post Bag 4, Ganeshkhind, Pune
University Campus, Pune, 411007, India*

J. Novak, M. Oertel

*LUTH, Observatoire de Paris, PSL Research University, CNRS, Université Paris Diderot,
Sorbonne Paris Cité, 5 place Jules Janssen, 92195 Meudon, France*

Electron captures by atomic nuclei in dense matter are among the most important processes governing the late evolution of stars, limiting in particular the stability of white dwarfs. Despite considerable progress in the determination of the equation of state of dense Coulomb plasmas, the threshold electron Fermi energies are still generally estimated from the corresponding Q values in vacuum. Moreover, most studies have focused on nonmagnetized matter. However, some white dwarfs are endowed with magnetic fields reaching 10^9 G. Even more extreme magnetic fields might exist in super Chandrasekhar white dwarfs, the progenitors of overluminous type Ia supernovae like SN 2006gz and SN 2009dc. The roles of the dense stellar medium and magnetic fields on the onset of electron captures and on the structure of white dwarfs are briefly reviewed. New analytical formulas are derived to evaluate the threshold density for the onset of electron captures for arbitrary magnetic fields. Their influence on the structure of white dwarfs is illustrated by simple analytical formulas and numerical calculations.

Keywords: White dwarf; Chandrasekhar limit; Electron capture; Magnetic field.

1. Introduction

In 1926, the British physicist Ralph Fowler showed that the energy and the pressure of matter in the dense core of a white dwarf remain finite at zero temperature due to quantum mechanics. Considering that electrons are no longer bound to nuclei under such extreme conditions, he derived the equation of state of a degenerate electron Fermi gas¹. Another British physicist, Edmund Clifton Stoner, calculated the structure of white dwarfs with uniform density in 1929². The same year, Wil-

helm Anderson, a physicist at the University of Tartu in Estonia, first stressed the importance of taking into account the relativistic motion of electrons³. He showed that the mass of a white dwarf tends to some finite value as the electron concentration increases, namely $M_{\text{And}} \sim 0.69M_{\odot}$ assuming an electron fraction $y_e = 0.4$ (with M_{\odot} the mass of the Sun). Improving Anderson's approximate treatment, Stoner⁴ found $M_{\text{St}} \simeq 1.10M_{\odot}$. Soon afterwards, the young Indian physicist Subrahmanyan Chandrasekhar solved the hydrostatic equilibrium equations for an ultrarelativistic electron Fermi gas using the theory of polytropes⁵. His numerical result, $M_{\text{Ch}} \simeq 0.91M_{\odot}$ (for $y_e = 0.4$), thus differed by less than 20% from that obtained earlier by Stoner, a remarkably close agreement as pointed out by Chandrasekhar himself. A year later, the Russian physicist Lev Landau showed that any degenerate star has a maximum mass, which can be expressed in terms of the fundamental constants as

$$M_{\text{L}} = 3.1 \frac{m_{\text{P}}^3}{m^2} y_e^2, \quad (1)$$

where we have introduced the Planck mass

$$m_{\text{P}} = \sqrt{\frac{\hbar c}{G}}, \quad (2)$$

(\hbar is the Planck-Dirac constant, c is the speed of light, G is the constant of gravitation) and m is the average mass per nucleon. Incidentally, such a scaling was already apparent in Stoner's analysis of a uniform density star. Combining his equations (17) and (19b) leads to

$$M_{\text{St}} = \frac{15\sqrt{5\pi}}{16} \frac{m_{\text{P}}^3}{m^2} y_e^2. \quad (3)$$

Landau however did not believe in the physical reality of this limit and even invoked some violation of the laws of quantum mechanics inside massive stars to prevent them from collapsing (see Ref. 6 for a historical perspective on Landau's contribution). As early as 1928, the process by which atoms are crushed at high densities was actually discussed by the Russian physicist Yakov Frenkel⁷. More importantly, he calculated the equation of state of an electron Fermi gas for an arbitrary degree of relativistic motion as well as the correction due to electrostatic interactions between electrons and atomic nuclei. He also studied the conditions for which incompressible "superdense stars" can exist and derived indirectly the mass limit. Correcting for an error in his expression for the gravitational energy^a and neglecting the electrostatic correction lead to the same result as the one published by Stoner in 1930. Frenkel's pioneer work remained unnoticed during several decades, and is still not very well-known today⁸.

The analyses of Anderson and Stoner showed that the maximum mass of white dwarfs is only reached asymptotically when the electron concentration tends to

^athe factor 5/3 in his key equation (19a) should read 3/5; this error goes back to his incorrect expression (18) for the gravitational energy.

infinity and the stellar radius goes to zero. This conclusion was later confirmed by the numerical calculations of Chandrasekhar for more realistic density profiles⁹. However, soon after the discovery of the neutron by James Chadwick in 1932, it was realized that matter becomes predominantly composed of neutrons at high densities^{10,11}. In December 1933, during a meeting of the American Physical Society at Stanford, Wilhelm Baade and Fritz Zwicky predicted the existence of *neutron stars* formed from the catastrophic gravitational collapse of stars during supernova explosions¹². Baade and Zwicky were apparently unaware of the studies about white dwarfs. The connection was first made by Landau¹³ and Gamow¹⁴. At a conference in Paris in 1939, Chandrasekhar also pointed out¹⁵:

If the degenerate core attains sufficiently high densities, the protons and electrons will combine to form neutrons. This would cause a sudden diminution of pressure resulting in the collapse of the star to a neutron core.

In 1956, the French physicist Evry Schatzman¹⁶ showed that the central density of white dwarfs is limited by the onset of electron captures by nuclei, implying that the radius of the most massive white dwarfs remains *finite*. Detailed calculations of the structure of white dwarfs taking into account matter neutronization were performed at the end of the 1950s and at the beginning of the 1960s^{17–19}. Electron captures are now known to play a key role in the late stages of stellar evolution (see Ref. 20 for a recent review).

Although the electrostatic correction to the equation of state of an electron Fermi gas was calculated long ago⁷ (see Ref. 21 and references therein for the latest developments on the equation of state of dense Coulomb plasmas), the threshold electron Fermi energy μ_e for the onset of electron captures by nuclei is still generally estimated from the corresponding Q value in *vacuum*. Moreover, the presence of magnetic fields is usually ignored. However, a significant fraction of white dwarfs have been found²² to have magnetic fields up to 10^9 G, and potentially much stronger fields may exist in their core²³. Moreover, it has been recently proposed that very massive so-called super-Chandrasekhar white dwarfs (with a mass $M \gtrsim 2M_\odot$) endowed with extremely strong magnetic fields could be the progenitors of overluminous type Ia supernovae like SN 2006gz and SN 2009dc^{24–26} (see also Refs. 27–30). The existence of such stars was actually first studied much earlier by Shul'man³¹, who found that the maximum mass of degenerate stars could be increased by two orders of magnitude if the magnetic field is strongly quantizing^{32,33}. However, the stability of such super Chandrasekhar white dwarfs will still be limited by electron captures^{34,35}. Detailed calculations of the global structure of these stars taking these processes into account have been carried out in Refs. 36,37.

In this paper, we review our recent studies of the role of electron-ion interactions and magnetic fields in the onset of electron captures in cold white-dwarf cores^{36,38}. We also present more accurate and more general formulas for the threshold density and pressure, applicable not only to nonmagnetic and strongly magnetized white

dwarfs but also to stars with intermediate magnetic field strengths. The impact of electron captures on the global structure of white dwarfs is discussed and new numerical results are presented.

2. Core of white dwarfs with magnetic fields

The core of a white dwarf consists of a dense Coulomb plasma of nuclei in a charge compensating background of relativistic electrons. Apart from carbon and oxygen (the primary ashes of helium burning), the core may contain other nuclei like helium^{39–41}, neon and magnesium⁴², or even iron^{43,44}. Iron white dwarfs could be formed from the explosive ignition of electron degenerate oxygen-neon-magnesium cores⁴⁵, or from failed detonation supernovae⁴⁶. For simplicity, we assume that the stellar core is made of only one type of nuclei with charge number Z and mass number A (see, e.g. Ref. 38 for the treatment of mixtures). We further suppose that the star has sufficiently cooled down such that thermal effects can be neglected.

Whereas nuclei with number density n_N exert a negligible pressure $P_N = 0$, they contribute to the mass density

$$\rho = n_N M'(A, Z), \quad (4)$$

where $M'(A, Z)$ denotes the ion mass including the rest mass of Z electrons and can be obtained from the experimental *atomic* mass $M(A, Z)$ by subtracting out the binding energy of the atomic electrons (see Eq. (A4) of Ref. 47). In principle, the presence of a magnetic field can have some effect on nuclei^{48,49}. However, the change of nuclear masses is negligible even for the strongest magnetic fields of order 10^{15} G expected in super Chandrasekhar white dwarfs^{29,36,50}.

To a very good approximation, electrons can be treated as an ideal Fermi gas. In the presence of a magnetic field, the electron motion perpendicular to the field is quantized into Landau-Rabi levels^{51,52}. Quantization effects on the equation of state are significant when B exceeds B_{rel} , where

$$B_{\text{rel}} \equiv \frac{m_e^2 c^3}{e \hbar} \approx 4.4 \times 10^{13} \text{ G}, \quad (5)$$

where m_e is the electron mass and e is the elementary electric charge. The expressions for the energy density \mathcal{E}_e and pressure P_e for arbitrary magnetic field strength can be found in Ref. 53.

The main correction to the ideal electron Fermi gas arises from the electron-ion interactions, as first shown by Frenkel⁷ (see e.g. Ref. 53 for a discussion of higher-order corrections). For pointlike ions embedded in a uniform electron gas with number density $n_e = Zn_N$ (from electric charge neutrality), the corresponding energy density is given by (see e.g. Chap. 2 of Ref. 53)

$$\mathcal{E}_L = C_M \left(\frac{4\pi}{3} \right)^{1/3} e^2 n_e^{4/3} Z^{2/3}, \quad (6)$$

where C_M is the Madelung constant. The contribution to the pressure is thus given by

$$P_L = n_e^2 \frac{d(\mathcal{E}_L/n_e)}{dn_e} = \frac{\mathcal{E}_L}{3}. \quad (7)$$

The pressure of the Coulomb plasma finally reads $P = P_e + P_L$.

In the following, we shall consider that ions are arranged in a body-centered cubic lattice since this configuration leads to the lowest energy⁵³. In this case, the Madelung constant is given by⁵⁴ $C_M = -0.895929255682$. According to the Bohr-van Leeuwen theorem⁵⁵, the electrostatic corrections (6) and (7) are independent of the magnetic field apart from a negligibly small contribution due to quantum zero-point motion of ions about their equilibrium position⁵⁶.

3. Onset of electron captures by nuclei in dense environments

The onset of electron captures by nuclei (A, Z) is formally determined by the same condition irrespective of the magnetic field strength by requiring the constancy of the Gibbs free energy per nucleon at fixed temperature and pressure³⁸. The threshold electron Fermi energy is found to first order in the fine-structure constant $\alpha = e^2/(\hbar c)$ from the condition:

$$\gamma_e + C_M \left(\frac{4\pi n_e}{3} \right)^{1/3} \alpha \lambda_e F(Z) = \gamma_e^\beta(A, Z), \quad (8)$$

$$F(Z) \equiv Z^{5/3} - (Z-1)^{5/3} + \frac{1}{3}Z^{2/3}, \quad (9)$$

$$\gamma_e^\beta(A, Z) \equiv -\frac{Q_{\text{EC}}(A, Z)}{m_e c^2} + 1, \quad (10)$$

where $\gamma_e \equiv \mu_e/(m_e c^2)$, $\lambda_e = \hbar/(m_e c)$ is the electron Compton wavelength, and we have introduced the Q -value (in vacuum) associated with electron capture by nuclei (A, Z) :

$$Q_{\text{EC}}(A, Z) = M'(A, Z)c^2 - M'(A, Z-1)c^2. \quad (11)$$

These Q -values can be obtained from the tabulated Q -values of β decay by the following relation:

$$Q_{\text{EC}}(A, Z) = -Q_\beta(A, Z-1). \quad (12)$$

In principle, the daughter nucleus may be in an excited state. However, such a transition would occur at a higher density.

In the absence of magnetic fields, the threshold condition (8) can be solved analytically⁵⁷. Recalling that the electron Fermi energy is given by

$$\mu_e = m_e c^2 \sqrt{1 + x_r^2}, \quad (13)$$

6

where $x_r = \lambda_e k_e$ and $k_e = (3\pi^2 n_e)^{1/3}$ is the electron Fermi wave number, the solution reads

$$x_r^\beta = \gamma_e^\beta \left\{ \sqrt{1 - \left[1 - \tilde{F}(Z)^2 \right] / (\gamma_e^\beta)^2 - \tilde{F}(Z)} \right\} \left[1 - \tilde{F}(Z)^2 \right]^{-1}, \quad (14)$$

with

$$\tilde{F}(Z) \equiv C_M \left(\frac{4}{9\pi} \right)^{1/3} \alpha F(Z). \quad (15)$$

The pressure $P_\beta(A, Z)$ at the onset of electron captures is given by

$$P_\beta(A, Z) = \frac{m_e c^2}{8\pi^2 \lambda_e^3} \left[x_r^\beta \left(\frac{2}{3} (x_r^\beta)^2 - 1 \right) \sqrt{1 + (x_r^\beta)^2} + \ln(x_r^\beta + \sqrt{1 + (x_r^\beta)^2}) \right] + \frac{C_M \alpha}{3} \left(\frac{4}{243\pi^7} \right)^{1/3} (x_r^\beta)^4 \frac{m_e c^2}{\lambda_e^3} Z^{2/3}. \quad (16)$$

The corresponding average mass density is found from Eq. (4) and is given by

$$\rho_\beta(A, Z) = \frac{M'(A, Z)}{Z} \frac{(x_r^\beta)^3}{3\pi^2 \lambda_e^3}. \quad (17)$$

Numerical results are summarized in Table 1 for nuclei expected to be found in the core of white dwarfs, using data from the 2020 Atomic Mass Evaluation⁵⁸. Fundamental constants were taken from NIST CODATA 2018^b. We have not considered helium since this element is expected to undergo pycnonuclear fusion in white-dwarf cores before capturing electrons.

Table 1. Dimensionless threshold electron Fermi energy $\gamma_e = \mu_e / (m_e c^2)$, mass density ρ_β and pressure P_β for the onset of electron captures by the given nuclei in unmagnetized white dwarfs.

	¹⁶ O	¹² C	²⁰ Ne	²⁴ Mg	⁵⁶ Fe
γ_e	22.0	27.8	15.2	12.2	8.74
ρ_β [g cm ⁻³]	2.06×10^{10}	4.16×10^{10}	6.81×10^9	3.51×10^9	1.37×10^9
P_β [dyn cm ⁻²]	2.73×10^{28}	6.99×10^{28}	6.21×10^{27}	2.56×10^{27}	6.46×10^{26}

In the presence of a magnetic field, the threshold condition (8) must be solved using the following relation between n_e and γ_e :

$$n_e = \frac{2B_\star}{(2\pi)^2 \lambda_e^3} \sum_{\nu=0}^{\nu_{\max}} g_\nu x_e(\nu), \quad (18)$$

$$x_e(\nu) = \sqrt{\gamma_e^2 - 1 - 2\nu B_\star}, \quad (19)$$

^b<https://physics.nist.gov/cuu/Constants/index.html>

where we have introduced $B_\star \equiv B/B_{\text{rel}}$, and the degeneracy $g_\nu = 1$ for $\nu = 0$ and $g_\nu = 2$ for $\nu \geq 1$. The index ν_{max} is the highest integer for which $\gamma_e^2 - 1 - 2\nu_{\text{max}}B_\star \geq 0$, i.e.

$$\nu_{\text{max}} = \left[\frac{\gamma_e^2 - 1}{2B_\star} \right], \quad (20)$$

where $[.]$ denotes the integer part.

In the weakly quantizing regime meaning that many Landau-Rabi levels are populated ($\nu_{\text{max}} \gg 1$), analytical solutions can be found. Remarking that the magnetic field enters explicitly in (8) only through the small electrostatic correction, the threshold electron Fermi energy is still approximately given by the solution in the absence of magnetic fields, namely $\gamma_e \approx \sqrt{1 + (x_r^\beta)^2}$ with x_r^β given by (14). Substituting in Eqs. (18) and (19), using the expansions (41) obtained in Ref. 59 leads to the following estimate for the density marking the onset of electron captures:

$$\rho_\beta(A, Z) \approx \frac{M'(A, Z)}{2\pi^2 Z \lambda_e^3} \left[\frac{2}{3} (\gamma_e^2 - 1)^{3/2} + (2B_\star)^{3/2} \zeta \left(\frac{-1}{2}, \left\{ \frac{\gamma_e^2 - 1}{2B_\star} \right\} \right) + \frac{B_\star^2}{6\sqrt{\gamma_e^2 - 1}} \right], \quad (21)$$

where $\zeta(z, q)$ is the Hurwitz zeta function defined by

$$\zeta(z, q) = \sum_{\nu=0}^{+\infty} \frac{1}{(\nu + q)^z} \quad (22)$$

for $\Re(z) > 1$ and by analytic continuation to other $z \neq 1$ (excluding poles $\nu + q = 0$), and $\{.\}$ in the argument denotes the fractional part. The first term in Eq. (21) represents the threshold density in the absence of magnetic field. The second term accounts for magnetic oscillations while the last term is a higher-order correction. The expression for the associated pressure is more involved. Using Eqs. (41), (43)

8

and (44) of Ref. 59 yields^c

$$\begin{aligned}
P_\beta(A, Z) \approx & \frac{m_e c^2}{4\pi^2 \lambda_e^3} \left\{ \frac{1}{2} \left(1 - 2B_\star + \frac{2B_\star^2}{3} \right) \log \left(\frac{\gamma_e + \sqrt{2B_\star + \gamma_e^2 - 1}}{1 + \sqrt{2B_\star}} \right) \right. \\
& - \frac{1}{2} \left(\gamma_e \sqrt{2B_\star + \gamma_e^2 - 1} - \sqrt{2B_\star} \right) + \frac{1}{3} \left(\gamma_e \sqrt{2B_\star + \gamma_e^2 - 1}^3 - \sqrt{2B_\star}^3 \right) \\
& + B_\star \left(\operatorname{arccosh} \gamma_e - \gamma_e \sqrt{\gamma_e^2 - 1} \right) - (2B_\star)^{5/2} \int_0^{+\infty} \frac{\tilde{\zeta}_3(-1/2, q+1)}{\sqrt{1+2B_\star q}} dq \\
& + \frac{2(2B_\star)^{5/2}}{3\gamma_e} \zeta \left(\frac{-3}{2}, \left\{ \frac{\gamma_e^2 - 1}{2B_\star} \right\} \right) + \frac{2(2B_\star)^{7/2}}{15\gamma_e^3} \zeta \left(\frac{-5}{2}, \left\{ \frac{\gamma_e^2 - 1}{2B_\star} \right\} \right) \\
& + \frac{1}{240} \left(\frac{B_\star}{\gamma_e} \right)^4 + 4B_\star^2 \int_0^1 \zeta \left(\frac{-1}{2}, q \right) \zeta \left(\frac{1}{2}, q + \frac{1}{2B_\star} \right) dq \\
& + \frac{2}{3} \left(\frac{2}{3\pi} \right)^{1/3} C_M \alpha Z^{2/3} \left[\frac{2}{3} (\gamma_e^2 - 1)^{3/2} \right. \\
& \left. + (2B_\star)^{3/2} \zeta \left(\frac{-1}{2}, \left\{ \frac{\gamma_e^2 - 1}{2B_\star} \right\} \right) + \frac{B_\star^2}{6\sqrt{\gamma_e^2 - 1}} \right]^{4/3} \Big\}, \quad (23)
\end{aligned}$$

with

$$\tilde{\zeta}_3(z, q) = \zeta(z, q) - \frac{1}{z-1} q^{-z+1} - \frac{1}{2} q^{-z} - \frac{z}{12} q^{-z-1}. \quad (24)$$

An analytical solution also exists in the strongly quantizing regime whereby electrons are all confined to the lowest Landau-Rabi level ($\nu_{\max} = 0$). Introducing

$$\bar{F}(Z, B_\star) \equiv \frac{1}{3} C_M \alpha F(Z) \left(\frac{2B_\star}{3\pi} \right)^{1/3} < 0, \quad (25)$$

$$v \equiv \frac{\gamma_e^\beta}{2|\bar{F}(Z, B_\star)|^{3/2}}, \quad (26)$$

the solutions are given by the following formulas⁶⁰:

$$\gamma_e = \begin{cases} 8|\bar{F}(Z, B_\star)|^{3/2} \cosh^3 \left(\frac{1}{3} \operatorname{arccosh} v \right) & \text{if } v \geq 1, \\ 8|\bar{F}(Z, B_\star)|^{3/2} \cos^3 \left(\frac{1}{3} \arccos v \right) & \text{if } 0 \leq v < 1. \end{cases} \quad (27)$$

The threshold pressure and density are respectively given by:

$$\begin{aligned}
P_\beta(A, Z, B_\star) = & \frac{B_\star m_e c^2}{4\pi^2 \lambda_e^3} \left[\gamma_e \sqrt{\gamma_e^2 - 1} - \ln \left(\sqrt{\gamma_e^2 - 1} + \gamma_e \right) \right. \\
& \left. + \frac{C_M \alpha}{3} \left(\frac{16B_\star Z^2}{3\pi} \right)^{1/3} (\gamma_e^2 - 1)^{2/3} \right], \quad (28)
\end{aligned}$$

^cIn the notations of Ref. 59, the electron contribution to the pressure can be directly obtained from the grand potential density by $P_e = -\omega_0^{(\text{mon})} - \omega_0^{(\text{osc})}$. The total pressure is found by adding the electrostatic correction (7) using the expansion for the electron density.

$$\rho_\beta(A, Z, B_\star) = \frac{B_\star}{2\pi^2\lambda_e^3} \frac{M'(A, Z)}{Z} \sqrt{\gamma_e^2 - 1}. \quad (29)$$

Let us recall that Eq. (27) is only valid if all electrons lie in the lowest Landau-Rabi level, i.e. if their Fermi energy does not exceed $\gamma_e = \sqrt{1 + 2B_\star} \approx \sqrt{2B_\star}$ or equivalently if their density does not exceed $n_e = B_\star^{3/2}/(\sqrt{2}\pi^2\lambda_e^3)$ using Eqs. (18) and (19). This condition translates into a lower bound for the magnetic field $B_\star \geq B_{\star 1}$. To find $B_{\star 1}$, we substitute the above expressions for γ_e and n_e in Eq. (8). This leads to

$$B_{\star 1} = \frac{(\gamma_e^\beta)^2}{2} \left[1 + \frac{C_M \alpha}{(3\pi)^{1/3}} F(Z) \right]^{-2}. \quad (30)$$

Values for some nuclei are summarized in Table 2. For magnetic field strength $B_\star \lesssim B_{\star 1}$, the threshold condition (8) must be solved numerically.

Table 2. Magnetic field strength in units of B_{rel} above which electrons are confined to the lowest Rabi level when captured by the given nuclei.

^{16}O	^{12}C	^{20}Ne	^{24}Mg	^{56}Fe
240	384	115	74.1	37.8

Full results for different nuclei expected to be found in white-dwarf cores are shown in Figs. 1 and 2. Changes in the occupation of Rabi levels as the magnetic field is increased lead to typical oscillations of the threshold density ρ_β : the onset of electron captures can thus be shifted to either lower or higher density as compared to unmagnetized matter. The lowest value is reached for $B_\star = B_{\star 1}$ and lies about 25% below the threshold density in the absence of magnetic fields irrespective of the composition (this can be easily shown by taking the ratio of Eqs. (29) and (17) using (30) and ignoring all terms in α). In the strongly quantizing regime, ρ_β is unbound from above and increases almost linearly with B_\star .

4. Global structure of white dwarfs

The core of a white dwarf is expected to be surrounded by a helium mantle and an hydrogen envelope. Their contribution to the mass of the star cannot exceed $\sim 1\%$ to avoid a thermonuclear runaway. For simplicity, we will ignore these layers here.

In the model originally considered by Chandrasekhar⁵, the interior of a white dwarf was described using the equation of state of an ideal electron Fermi gas. The composition, assumed to be uniform, was only included throughout the charge neutrality condition. In the ultrarelativistic limit, the resulting equation of state reduces to the polytropic form $P \approx K_0 \rho^{4/3}$ with

$$K_0 = \frac{\hbar c (3\pi^2)^{1/3}}{4} \left(\frac{Z}{M'(A, Z)} \right)^{4/3}. \quad (31)$$

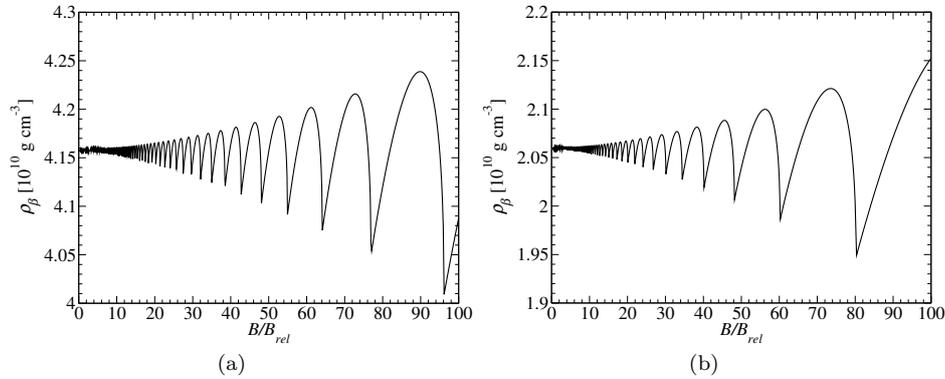


Fig. 1. Threshold density for the onset of electron captures by nuclei as a function of the magnetic field strength in units of the characteristic field (5). (a) Results for ^{12}C . (b) Results for ^{16}O .

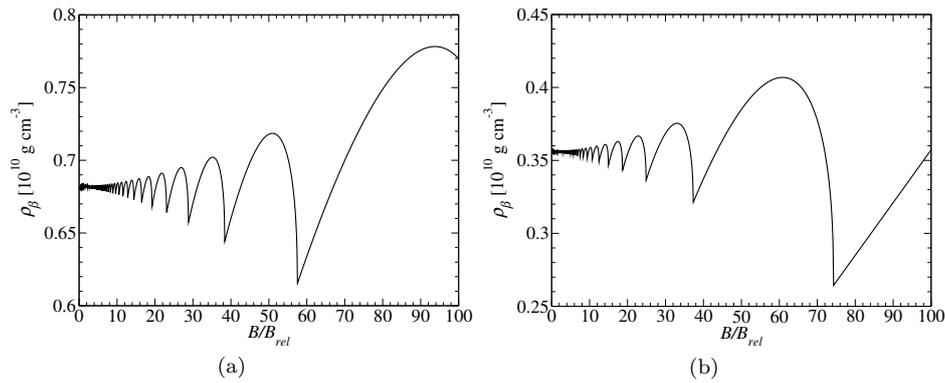


Fig. 2. Same as Fig. 1 for (a) ^{20}Ne and (b) ^{24}Mg .

The mass and radius of a white dwarf with central density ρ_c can be deduced from the theory of polytropes⁶¹

$$M_{\text{Ch}} = 4\pi \left(\frac{K_0}{\pi G} \right)^{3/2} \xi_1^2 |\theta'(\xi_1)|, \quad (32)$$

$$R_{\text{Ch}} = \sqrt{\frac{K_0}{\pi G}} \frac{\xi_1}{\rho_c^{1/3}} \quad (33)$$

respectively, where $\xi_1 \simeq 6.89685$ and $\xi_1^2 |\theta'(\xi_1)| \simeq 2.01824$. Substituting the expression for K_0 thus yields

$$M_{\text{Ch}} = \frac{\sqrt{3\pi}}{2} \xi_1^2 |\theta'(\xi_1)| \frac{m_{\text{P}}^3}{m^2} y_e^2 \simeq 3.09798 \frac{m_{\text{P}}^3}{m^2} y_e^2, \quad (34)$$

$$R_{\text{Ch}} = \frac{\sqrt{3\pi}}{2} \xi_1 \lambda_e \frac{m_{\text{P}}}{m} \frac{y_e}{x_{r,c}} \simeq 10.5866 \lambda_e \frac{m_{\text{P}}}{m} \frac{y_e}{x_{r,c}}, \quad (35)$$

where

$$m \equiv \frac{M'(A, Z)}{A}, \quad (36)$$

and $x_{r,c}$ denotes the relativity parameter at the density ρ_c . Equation (34) coincides with the maximum mass because the ultrarelativistic regime is only valid at high densities such that the relativity parameter in the central core of the star satisfies $x_{r,c} \gg 1$. In the limit $x_{r,c} \rightarrow +\infty$, the radius R_{Ch} vanishes.

The electrostatic corrections (6) and (7) can be easily taken into account by simply renormalizing the constant K_0 as

$$K = K_0 \left[1 + \alpha \frac{8C_M}{6} \left(\frac{4}{9\pi} \right)^{1/3} Z^{2/3} \right]. \quad (37)$$

The mass and radius thus become^d

$$M = \left[1 + \alpha \frac{8C_M}{6} \left(\frac{4}{9\pi} \right)^{1/3} Z^{2/3} \right]^{3/2} M_{\text{Ch}} < M_{\text{Ch}}, \quad (38)$$

$$R = R_{\text{Ch}} \left[1 + \alpha \frac{8C_M}{6} \left(\frac{4}{9\pi} \right)^{1/3} Z^{2/3} \right]^{1/2} < R_{\text{Ch}}. \quad (39)$$

This shows how the electron-ion interactions lower both the mass and the radius. It can be seen that the radius of the most massive white dwarfs still vanishes in the limit $x_{r,c} \rightarrow +\infty$. However, as discussed earlier, nuclei in the white dwarf core will capture electrons as soon as the central density ρ_c exceeds the threshold density ρ_β . The daughter nuclei are generally unstable against a second electron capture. The transition is accompanied by a discontinuous increase of density given by

$$\frac{\Delta\rho}{\rho_\beta} = \frac{Z}{Z-2} \frac{M'(A, Z-2)}{M'(A, Z)} \left[1 + \alpha C_M \left(\frac{4}{9\pi} \right)^{1/3} \left(Z^{2/3} - (Z-2)^{2/3} \right) \frac{\sqrt{1+x_r^2}}{x_r} \right] - 1, \quad (40)$$

where x_r is given by Eq. (14). The density jump is about 50% for carbon, 33% for oxygen, 25% for neon, 20% for magnesium, and 8.2% for iron.

Because these reactions occur at the same pressure, the adiabatic index defined by

$$\Gamma = \frac{d \log P}{d \log \rho} \quad (41)$$

therefore vanishes thus making the star unstable. In the limit of ultrarelativistic electrons, the average threshold density and pressure reduce to

$$\rho_\beta(A, Z) \approx \frac{M'(A, Z)}{Z} \frac{\mu_e^\beta(A, Z)^3}{3\pi^2(\hbar c)^3} \left[1 + \alpha C_M \left(\frac{4}{9\pi} \right)^{1/3} F(Z) \right]^{-3}, \quad (42)$$

^dSuch kind of scaling was briefly mentioned in Ref. 19 through an effective mean molecular weight per electron.

$$P_\beta(A, Z) \approx \frac{\mu_e^\beta(A, Z)^4}{12\pi^2(\hbar c)^3} \left[1 + 4C_M \alpha Z^{2/3} \left(\frac{4}{243\pi} \right)^{1/3} \right] \left[1 + \alpha C_M \left(\frac{4}{9\pi} \right)^{1/3} F(Z) \right]^{-4}. \quad (43)$$

Substituting Eq. (42) in (39) using (35) leads to the following lower bound for the radius of a white dwarf:

$$R_{\min} = \frac{\sqrt{3\pi}}{2} \xi_1 \lambda_e \frac{m_P}{m} \frac{y_e}{\gamma_e^\beta(A, Z)} \left[1 + \alpha C_M \left(\frac{4}{9\pi} \right)^{1/3} F(Z) \right] \times \left[1 + \alpha \frac{8C_M}{6} \left(\frac{4}{9\pi} \right)^{1/3} Z^{2/3} \right]^{1/2}. \quad (44)$$

The factors in square brackets account for the electron-ion interactions: the first arises from the shift in the threshold density for the onset of electron captures whereas the second is due to the correction to the equation of state. Both factors lead to a reduction of the radius. Results of Eq. (44) are summarized in Table 3.

Table 3. Minimum radius (in km) of nonmagnetic stable white dwarfs.

¹² C	¹⁶ O	²⁰ Ne	²⁴ Mg	⁵⁶ Fe
958	1209	1743	2168	2791

The mass remains unchanged since it does not depend on the density and is still given by Eq. (38). However, departure from the polytropic equation of state $P = K\rho^{4/3}$ and the fact that the central density ρ_c is finite induce a slight reduction of the maximum mass. Following the perturbative approach described in Chapter 6 of Ref. 62 and based on the minimization of some approximation for the total energy of the star, we find

$$\frac{\delta M}{M} \approx -\frac{k_3}{k_2} \frac{3\pi}{(\gamma_e^\beta)^2} \left(\frac{3}{2\xi_1^4 |\theta'(\xi_1)|^2} \right)^{1/3} \left[1 + \alpha \frac{8C_M}{6} \left(\frac{4}{9\pi} \right)^{1/3} Z^{2/3} \right]^{-1} \times \left[1 + \alpha C_M \left(\frac{4}{9\pi} \right)^{1/3} F(Z) \right]^2 \quad (45)$$

where $k_2 = 0.639001$ and $k_3 = 0.519723$. Results are summarized in Table 4. The influence of electron captures and electron-ion interactions are all the more important that matter contains heavier elements: whereas the overall reduction of the Chandrasekhar mass M_{Ch} amounts to 3% for carbon, it reaches 13% for iron.

The stability of a white dwarf can be further limited by general relativity, as first shown by Kaplan⁶³. The critical density above which the stellar core becomes unstable can be estimated from the minimization of the total energy. Including the electrostatic correction in Eq.(6.10.28) of Ref. 62 we find

$$\rho_{\text{GR}} = \frac{16k_3(k_2)^2}{(3\pi^2)^{2/3}k_4(k_1)^2} \frac{M'(A, Z)^2}{Z^2 \lambda_e^3 m_e} \left[1 + \alpha \frac{8C_M}{6} \left(\frac{4}{9\pi} \right)^{1/3} Z^{2/3} \right]^{-2} \text{ g cm}^{-3}, \quad (46)$$

Table 4. Maximum mass (in solar units) of nonmagnetic white dwarfs for an ultra-relativistic electron Fermi gas (first line), with electrostatic correction (second line) and electron captures (third line).

^{12}C	^{16}O	^{20}Ne	^{24}Mg	^{56}Fe
1.456	1.457	1.457	1.458	1.259
1.424	1.418	1.411	1.406	1.184
1.413	1.401	1.377	1.353	1.095

where $k_1 = 1.75579$ and $k_4 = 0.918294$. Because $C_M < 0$, electron-ion interactions thus make the star more stable. We have also solved the Tolman-Oppenheimer-Volkoff^{64,65} equations for calculating the whole sequence of white dwarfs in full general relativity. In this way, we have determined more accurately the central (mass-energy) density ρ_{GR} at which $dM/d\rho_{\text{GR}} = 0$ marking the onset of instability. The hydrostatic equilibrium equations were integrated from the center of the star up to the point where electrons start to bind to nuclei at the density $\rho_{\text{eip}} = ZM'(A, Z)/a_0^3$ with a_0 the Bohr radius. Results are collected in Table 5. The values are systematically lower than those estimated from Eq. (46). Comparing Tables 1 and 5 shows that the central density is limited by general relativity rather than electron captures in carbon white dwarfs. Their mass-density relation is plotted in Fig. 3. The minimum radii and maximum masses of white dwarfs with different composition are indicated in Tables 6 and 7 respectively (note that the mass and radius of carbon white dwarfs at the onset of electron captures are respectively $1.484M_{\odot}$ and 855 km). For comparison, results obtained by solving numerically the Newtonian hydrostatic equilibrium equations are also given. Examining Tables 3 and 6 reveals that the polytropic approximation is more reliable for estimating the maximum mass than the minimum radius.

Table 5. Highest density ρ_{GR} (in g cm^{-3}) in nonmagnetic stable white dwarfs in general relativity, as calculated by minimization of the approximate total energy (first line) and by solving the hydrostatic equilibrium equations (second line).

^{16}O	^{12}C	^{20}Ne	^{24}Mg	^{56}Fe
2.73×10^{10}	2.72×10^{10}	2.75×10^{10}	2.76×10^{10}	3.31×10^{10}
2.39×10^{10}	2.40×10^{10}	2.42×10^{10}	2.44×10^{10}	2.93×10^{10}

The influence of a very strong magnetic field on the structure of white dwarfs was studied in Ref. 24 within the theory of polytropes making use of the fact that $P \propto \rho^2$ in the strongly quantizing regime. However, it was soon realized that this assumption is unrealistic and that the influence of the magnetic field itself on the stellar structure cannot be ignored^{27,34,66–68}. Moreover, the magnetic-field config-

Table 6. Minimum radius (in km) of nonmagnetic stable white dwarfs in Newtonian theory (first line) and general relativity (second line).

^{12}C	^{16}O	^{20}Ne	^{24}Mg	^{56}Fe
857.7	1055	1447	1736	2082
1010	1052	1444	1732	2079

Table 7. Maximum mass (in solar units) of nonmagnetic stable white dwarfs in Newtonian theory (first line) and general relativity (second line).

^{12}C	^{16}O	^{20}Ne	^{24}Mg	^{56}Fe
1.414	1.403	1.382	1.363	1.118
1.383	1.378	1.366	1.350	1.111

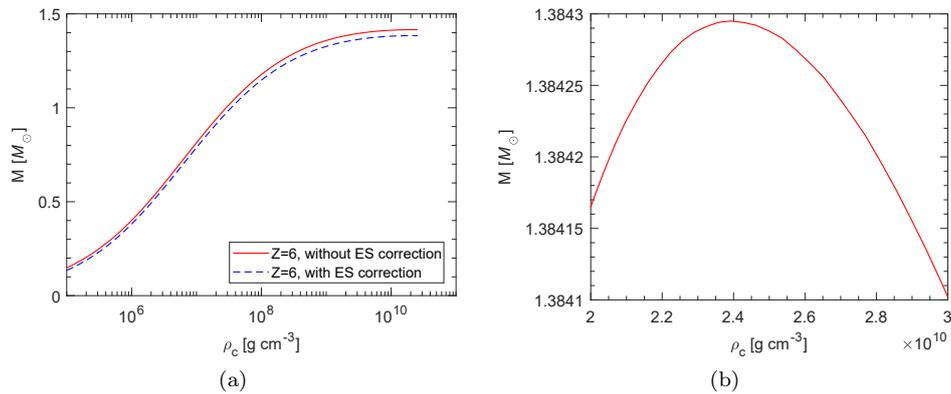


Fig. 3. Gravitational mass in solar masses versus central (mass-energy) density in g cm^{-3} of carbon white dwarfs in general relativity: (a) comparing results with and without electrostatic corrections, (b) closer view of results with electrostatic corrections around the critical point.

uration inside the star should be calculated from Maxwell's equations consistently with the stellar equilibrium equations. For all these reasons, the structure of magnetic white dwarfs is not easily amenable to a simple analytical treatment.

To study the influence of strong magnetic fields and the role of electron captures in white dwarfs, we have thus computed fully self-consistently numerical solutions of the Einstein-Maxwell equations using the LORENE library⁶⁹, suitably extended to allow for magnetic-field dependent equations of state and magnetization effects⁷⁰. We have found that purely poloidal magnetic fields of order 10^{14} G lead to super Chandrasekhar white dwarfs with a mass $\sim 2M_{\odot}$. Although such magnetic fields

have been found to have a rather small influence on the equation of state, they induce extreme stellar deformations with the most massive white dwarfs adopting a donut-like shape³⁶. Similarly to nonmagnetic white dwarfs, electron captures limit the maximum mass and the minimum radius of magnetic white dwarfs, as summarized in Table 8. However, the distortion of the star induced by magnetic fields tends to lower their density. For the most extreme configurations, the maximum density thus lies below the threshold density for the onset of electron captures. The mass-radius relations for magnesium and neon white dwarfs are plotted in Fig. 4.

Table 8. Maximum mass (in solar units) of magnetic white dwarfs, as determined by extreme deformations or electron captures (values in parentheses) for different magnetic moments \mathcal{M} in A m^2 .

\mathcal{M}	^{12}C	^{16}O	^{20}Ne	^{24}Mg
10^{33}	1.41 (1.41)	1.41 (1.40)	1.40 (1.38)	1.39 (1.38)
5×10^{33}	1.60 (1.50)	1.59 (1.46)	1.59 (1.41)	1.58 (1.36)
10^{34}	2.00 (1.86)	1.97 (1.67)	1.97 (1.51)	1.96 (1.45)
2×10^{34}	1.99 (1.99)	1.96 (1.96)	1.97 (1.95)	1.95 (1.73)
3×10^{34}	1.96 (1.96)	1.94 (1.94)	1.98 (1.98)	1.97 (1.97)

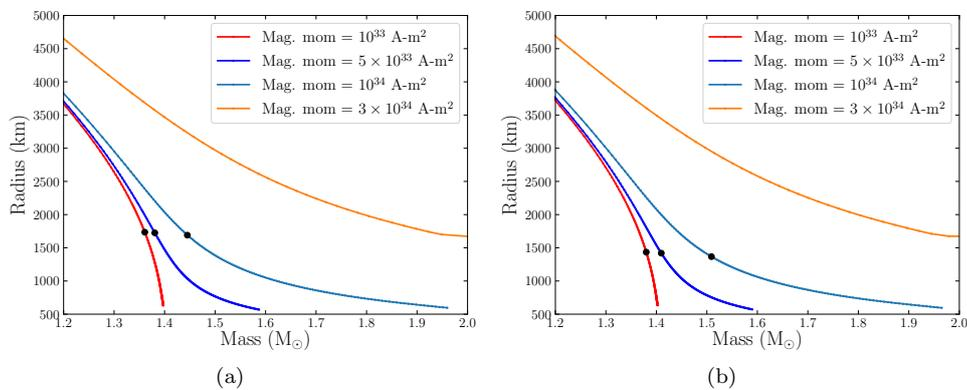


Fig. 4. Radius (in km) versus gravitational mass (in solar units) of white dwarfs for different magnetic moments: (a) for ^{24}Mg , (b) for ^{20}Ne . The onset of electron captures is marked by a filled circle.

The global stability criterion $\partial M/\partial \rho > 0$ still remains valid for magnetic white dwarfs provided the derivatives are evaluated for a fixed magnetic moment \mathcal{M} . As shown in Fig. 5, this instability is entirely removed by the presence of strong magnetic fields. In other words, the magnetic field makes the star more stable. In particular, the maximum mass of magnetic white dwarfs made of carbon is not limited by general relativity as their nonmagnetic relatives but by electron captures.

For magnetic white dwarfs to be the progenitors of overluminous type Ia supernova, i.e. to have masses $\sim 2M_{\odot}$, their magnetic field must be strong enough. Their minimum observable polar magnetic fields are indicated in Table 9 for different compositions. In all cases, the magnetic dipole moment is $3 \times 10^{34} \text{ A m}^2$.

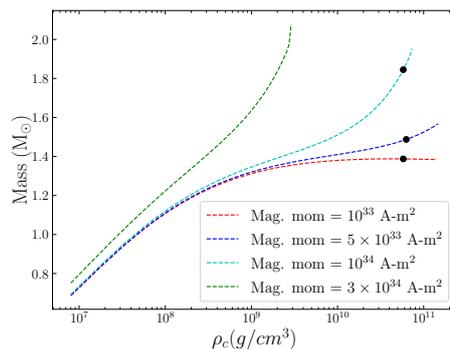


Fig. 5. Gravitational mass (in solar masses) versus central (mass-energy) density in g cm^{-3} of carbon white dwarfs in general relativity with given magnetic moments. The onset of electron captures is marked by a filled circle.

Table 9. Polar magnetic field (in 10^{13} G) of white dwarfs with $\mathcal{M} = 3 \times 10^{34} \text{ A m}^2$.

^{12}C	^{16}O	^{20}Ne	^{24}Mg
2.73	2.55	2.89	2.85

5. Conclusions

The stability of white dwarfs is limited by the onset of electron captures by nuclei in their core. We have presented very accurate analytical formulas for calculating the threshold electron Fermi energy, mass density and pressure in cold dense Coulomb plasmas with magnetic fields, taking into account Landau-Rabi quantization of electron motion. In particular, the density exhibits typical quantum oscillations associated with the filling of energy levels. As a consequence, electron captures in magnetic white dwarfs may occur at a lower or higher density than in their nonmagnetic relatives depending on the magnetic field strength. The lowest possible density is found to lie about 25% below its value in the absence of magnetic field essentially independently of the composition. On the contrary, the density is not

limited from above and increases almost linearly with the magnetic field strength in the strongly quantizing regime.

Taking into account electron-ion interactions using the polytropic approximation $P \approx K\rho^{4/3}$ with K given by Eq. (37), we have explicitly shown how electron captures alter the maximum mass of nonmagnetic white dwarfs and set a lower limit to their radius. We have also solved numerically the hydrostatic equilibrium equations using the full equation of state, both in Newtonian theory and in general relativity. We have found that electron captures reduce the maximum mass of white dwarfs by 3-13% compared to the Chandrasekhar model.

Solving the Einstein-Maxwell equations taking into account the magnetization of dense matter, we have found that white dwarfs with purely poloidal magnetic fields can be significantly more massive than their nonmagnetic relatives. We have also shown that the presence of strong magnetic fields makes the star more stable. The maximum mass of magnetic white dwarfs (including those made of carbon) is thus solely limited by electron captures. In turn, the large stellar deformations induced by the strongest magnetic fields lower the stellar density below the electron capture threshold. White dwarfs with polar magnetic fields exceeding 10^{13} G could thus be massive enough to explain overluminous type Ia supernova independently of the composition of their core. On the other hand, a purely poloidal magnetic-field configuration is unstable. The magnetic field in super Chandrasekhar white dwarfs is expected to have both poloidal and toroidal components. The question as to whether such stars can exist still remains open.

Although the present study was focused on white dwarfs, it may be also of interest for neutron stars as electron captures by nuclei constituting the outer crust of magnetars may explain their persistent luminosity and outbursts⁷¹. The general analytical formulas for the threshold density and pressure could thus be applied to determine the precise locations of these reactions.

Acknowledgments

The work of N.C. was financially supported by F.R.S.-FNRS under Grant No. IISN 4.4502.19. L. P. is a FRIA grantee of F.R.S.-FNRS. This work was also supported by COST CA16214 and the CNRS International Research Project “Origine des éléments lourds dans l’univers: Astres Compacts et Nucléosynthèse (ACNu)”.

References

1. R. H. Fowler, On dense matter, *MNRAS* **87**, 114 (December 1926).
2. E. C. Stoner, V. the limiting density in white dwarf stars, *Philos. Mag.* **7**, 63 (1929).
3. W. Anderson, Über die Grenzdichte der Materie und der Energie, *Z. Phys.* **56**, 851 (November 1929).
4. E. C. Stoner, Lxxxvii. the equilibrium of dense stars, *Philos. Mag.* **9**, 944 (1930).
5. S. Chandrasekhar, The Maximum Mass of Ideal White Dwarfs, *ApJ* **74**, p. 81 (July 1931).

6. D. G. Yakovlev, P. Haensel, G. Baym and C. Pethick, Lev Landau and the concept of neutron stars, *Physics Uspekhi* **56**, 289 (March 2013).
7. J. Frenkel, Zur wellenmechanischen Theorie der metallischen Leitfähigkeit, *Z. Phys.* **47**, 819 (November 1928).
8. D. G. Yakovlev, The article by Ya I Frenkel' on 'binding forces' and the theory of white dwarfs, *Physics Uspekhi* **37**, 609 (June 1994).
9. S. Chandrasekhar, The highly collapsed configurations of a stellar mass (Second paper), *MNRAS* **95**, 207 (January 1935).
10. T. E. Sterne, The equilibrium theory of the abundance of the elements: a statistical investigation of assemblies in equilibrium in which transmutations occur, *MNRAS* **93**, p. 736 (June 1933).
11. F. Hund, Materie unter sehr hohen Drucken und Temperaturen, *Ergebnisse der exakten Naturwissenschaften* **15**, p. 189 (January 1936).
12. W. Baade and F. Zwicky, Minutes of the stanford meeting, december 15-16, 1933, *Phys. Rev.* **45**, 130 (Jan 1934).
13. L. Landau, Origin of Stellar Energy, *Nature* **141**, 333 (February 1938).
14. G. Gamow, Physical Possibilities of Stellar Evolution, *Phys. Rev.* **55**, 718 (April 1939).
15. S. Chandrasekhar, The White Dwarfs and Their Importance for Theories of Stellar Evolution, in *Conférences du Collège de France, Colloque International d'Astrophysique III, 17-23 Juillet 1939*, 1941.
16. E. Schatzman, Influence of the nucleon-electron equilibrium on the internal structure of white dwarfs, *Astronomiceskij Zhurnal* **33**, p. 800 (1956).
17. E. Schatzman, *White Dwarfs* (North-Holland Publishing Company, 1958).
18. B. K. Harrison, M. Wakano and J. A. Wheeler, Matter-energy at high density: end point of thermonuclear evolution, in *Onzième Conseil de Physique Solvay, Stoops, Brussels*, 1958.
19. T. Hamada and E. E. Salpeter, Models for Zero-Temperature Stars., *ApJ* **134**, p. 683 (November 1961).
20. K. Langanke, G. Martínez-Pinedo and R. G. T. Zegers, Electron capture in stars, *Rep. Prog. Phys.* **84**, p. 066301 (June 2021).
21. A. S. Jermyn, J. Schwab, E. Bauer, F. X. Timmes and A. Y. Potekhin, Skye: A Differentiable Equation of State, *ApJ* **913**, p. 72 (May 2021).
22. L. Ferrario, D. de Martino and B. T. Gänsicke, Magnetic White Dwarfs, *Space Sci. Rev.* **191**, 111 (October 2015).
23. K. Fujisawa, S. Yoshida and Y. Eriguchi, Axisymmetric and stationary structures of magnetized barotropic stars with extremely strong magnetic fields deep inside, *MNRAS* **422**, 434 (May 2012).
24. U. Das and B. Mukhopadhyay, New Mass Limit for White Dwarfs: Super-Chandrasekhar Type Ia Supernova as a New Standard Candle, *Phys. Rev. Lett.* **110**, p. 071102 (February 2013).
25. U. Das and B. Mukhopadhyay, GRMHD formulation of highly super-Chandrasekhar magnetized white dwarfs: stable configurations of non-spherical white dwarfs, *J. Cosmol. Astropart. P.* **2015**, p. 016 (May 2015).
26. S. Subramanian and B. Mukhopadhyay, GRMHD formulation of highly super-Chandrasekhar rotating magnetized white dwarfs: stable configurations of non-spherical white dwarfs, *MNRAS* **454**, 752 (November 2015).
27. P. Bera and D. Bhattacharya, Mass-radius relation of strongly magnetized white dwarfs: nearly independent of Landau quantization, *MNRAS* **445**, 3951 (December 2014).
28. B. Franzon and S. Schramm, Effects of strong magnetic fields and rotation on white

- dwarf structure, *Phys. Rev. D* **92**, p. 083006 (October 2015).
29. P. Bera and D. Bhattacharya, Mass-radius relation of strongly magnetized white dwarfs: dependence on field geometry, GR effects and electrostatic corrections to the EOS, *MNRAS* **456**, 3375 (March 2016).
 30. P. Bera and D. Bhattacharya, A perturbation study of axisymmetric strongly magnetic degenerate stars: the case of super-Chandrasekhar white dwarfs, *MNRAS* **465**, 4026 (March 2017).
 31. G. A. Shul'man, Degenerate equilibrium stellar configurations with a frozen-in magnetic field, *Sov. Astron.* **20**, p. 689 (December 1976).
 32. G. A. Shulman, Equilibrium Configurations of Degenerate Superstars in the Quantum Limit of a Frozen-In Magnetic Field, *Sov. Astron.* **33**, p. 393 (August 1989).
 33. G. A. Shulman, Equilibrium and Stability of Degenerate Stars with a Frozen-In Quantizing Magnetic Field, *Sov. Astron.* **36**, p. 398 (August 1992).
 34. N. Chamel, A. F. Fantina and P. J. Davis, Stability of super-Chandrasekhar magnetic white dwarfs, *Phys. Rev. D* **88**, p. 081301 (October 2013).
 35. N. Chamel, E. Molter, A. F. Fantina and D. P. Arteaga, Maximum strength of the magnetic field in the core of the most massive white dwarfs, *Phys. Rev. D* **90**, p. 043002 (August 2014).
 36. D. Chatterjee, A. F. Fantina, N. Chamel, J. Novak and M. Oertel, On the maximum mass of magnetized white dwarfs, *MNRAS* **469**, 95 (July 2017).
 37. E. Otoniel, B. Franzone, G. A. Carvalho, M. Malheiro, S. Schramm and F. Weber, Strongly Magnetized White Dwarfs and Their Instability Due to Nuclear Processes, *ApJ* **879**, p. 46 (July 2019).
 38. N. Chamel and A. F. Fantina, Electron capture instability in magnetic and nonmagnetic white dwarfs, *Phys. Rev. D* **92**, p. 023008 (July 2015).
 39. G. Nelemans and T. M. Tauris, Formation of undermassive single white dwarfs and the influence of planets on late stellar evolution, *A&A* **335**, L85 (July 1998).
 40. J. Liebert, P. Bergeron, D. Eisenstein, H. C. Harris, S. J. Kleinman, A. Nitta and J. Krzesinski, A Helium White Dwarf of Extremely Low Mass, *ApJ* **606**, L147 (May 2004).
 41. O. G. Benvenuto and M. A. De Vito, The formation of helium white dwarfs in close binary systems - II, *MNRAS* **362**, 891 (September 2005).
 42. K. Nomoto, Evolution of 8-10 solar mass stars toward electron capture supernovae. I - Formation of electron-degenerate O + Ne + Mg cores., *ApJ* **277**, 791 (February 1984).
 43. J. A. Panei, L. G. Althaus and O. G. Benvenuto, Mass-radius relations for white dwarf stars of different internal compositions, *A&A* **353**, 970 (January 2000).
 44. S. Catalán, I. Ribas, J. Isern and E. García-Berro, WD0433+270: an old Hyades stream member or an Fe-core white dwarf?, *A&A* **477**, 901 (January 2008).
 45. J. Isern, R. Canal and J. Labay, The Outcome of Explosive Ignition of ONeMg Cores: Supernovae, Neutron Stars, or "Iron" White Dwarfs?, *ApJ* **372**, p. L83 (May 1991).
 46. G. C. Jordan, H. B. Perets, R. T. Fisher and D. R. van Rossum, Failed-detonation Supernovae: Subluminous Low-velocity Ia Supernovae and their Kicked Remnant White Dwarfs with Iron-rich Cores, *ApJ* **761**, p. L23 (December 2012).
 47. D. Lunney, J. M. Pearson and C. Thibault, Recent trends in the determination of nuclear masses, *Rev. Mod. Phys.* **75**, 1021 (August 2003).
 48. D. Peña Arteaga, M. Grasso, E. Khan and P. Ring, Nuclear structure in strong magnetic fields: Nuclei in the crust of a magnetar, *Phys. Rev. C* **84**, p. 045806 (October 2011).
 49. M. Stein, J. Maruhn, A. Sedrakian and P. G. Reinhard, Carbon-oxygen-neon mass

- nuclei in superstrong magnetic fields, *Phys. Rev. C* **94**, p. 035802 (September 2016).
50. S. Subramanian and B. Mukhopadhyay, GRMHD formulation of highly super-Chandrasekhar rotating magnetized white dwarfs: stable configurations of non-spherical white dwarfs, *MNRAS* **454**, 752 (November 2015).
 51. I. I. Rabi, Das freie Elektron im homogenen Magnetfeld nach der Diracschen Theorie, *Z. Phys.* **49**, 507 (July 1928).
 52. L. Landau, Diamagnetismus der Metalle, *Z. Phys.* **64**, 629 (September 1930).
 53. P. Haensel, A. Y. Potekhin and D. G. Yakovlev, *Neutron Stars 1: Equation of state and structure* (Springer, 2007).
 54. D. A. Baiko, A. Y. Potekhin and D. G. Yakovlev, Thermodynamic functions of harmonic Coulomb crystals, *Phys. Rev. E* **64**, p. 057402 (November 2001).
 55. J. H. Van Vleck, *The Theory of Electric and Magnetic Susceptibilities* (Oxford University Press, London, 1932).
 56. D. A. Baiko, Coulomb crystals in the magnetic field, *Phys. Rev. E* **80**, p. 046405 (October 2009).
 57. N. Chamel and A. F. Fantina, Binary and ternary ionic compounds in the outer crust of a cold nonaccreting neutron star, *Phys. Rev. C* **94**, p. 065802 (Dec 2016).
 58. M. Wang, W. J. Huang, F. G. Kondev, G. Audi and S. Naimi, The AME 2020 atomic mass evaluation (II). Tables, graphs and references, *Chin. Phys. C* **45**, p. 030003 (March 2021).
 59. C. O. Dib and O. Espinosa, The magnetized electron gas in terms of Hurwitz zeta functions, *Nucl. Phys. B* **612**, 492 (October 2001).
 60. N. Chamel and Z. K. Stoyanov, Analytical determination of the structure of the outer crust of a cold nonaccreted neutron star: Extension to strongly quantizing magnetic fields, *Phys. Rev. C* **101**, p. 065802 (June 2020).
 61. S. Chandrasekhar, *An introduction to the study of stellar structure* (Dover, 1957).
 62. S. L. Shapiro and S. A. Teukolsky, *Black Holes, White Dwarfs, and Neutron Stars: The Physics of Compact Objects* (John Wiley & Sons, 1983).
 63. S. A. Kaplan, Sverkhplotnyè Zvezdy, *Naukovy Zapiski* **15**, 109 (1949).
 64. R. C. Tolman, Static Solutions of Einstein's Field Equations for Spheres of Fluid, *Phys. Rev.* **55**, 364 (February 1939).
 65. J. R. Oppenheimer and G. M. Volkoff, On Massive Neutron Cores, *Phys. Rev.* **55**, 374 (February 1939).
 66. R. Nityananda and S. Konar, Strong constraints on magnetized white dwarfs surpassing the Chandrasekhar mass limit, *Phys. Rev. D* **89**, p. 103017 (May 2014).
 67. J. G. Coelho, R. M. Marinho, M. Malheiro, R. Negreiros, D. L. Cáceres, J. A. Rueda and R. Ruffini, Dynamical Instability of White Dwarfs and Breaking of Spherical Symmetry Under the Presence of Extreme Magnetic Fields, *ApJ* **794**, p. 86 (October 2014).
 68. D. L. Cáceres, J. A. Rueda and R. Ruffini, On the stability of ultra-magnetized white dwarfs, *J. Korean Phys. Soc.* **65**, 846 (September 2014).
 69. E.ourgoulhon, P. Grandclément, J.-A. Marck, J. Novak and K. Taniguchi, LORENE: Spectral methods differential equations solver (August 2016).
 70. D. Chatterjee, T. Elghozi, J. Novak and M. Oertel, Consistent neutron star models with magnetic-field-dependent equations of state, *MNRAS* **447**, 3785 (March 2015).
 71. N. Chamel, A. F. Fantina, L. Suleiman, J.-L. Zdunik and P. Haensel, Heating in Magnetar Crusts from Electron Captures, *Universe* **7**, p. 193 (June 2021).